Forest Chemicals Review
www.forestchemicalsreview.com
ISSN: 1520-0191
September-October 2022 Page No. 1151– 1166
Article History: Received: 06 April 2022, Revised: 28 April 2022, Accepted: 04 May 2022, Publication: 31 May 2022

Research on Dynamic Characteristic of Unmanned Ship Propulsion System Based on Variable Shaft Angle

Liangxiong Dong*, Jian Liu, Qiang Yuan
Zhejiang Ocean University, Zhoushan, Zhejiang, China
*Corresponding Author.

Abstract:

The strong dynamic load of will make the motion characteristics of shafting change rapidly and even lead to the loss of navigability of the ship. In order to solve the problem of engineering application of reliability assessment and control of ship propulsion system on heavy sea, the motion law between the driving shaft, the driven shaft and the shaft angle of the coupling is deduced by means of coordinate transformation method. Then, a simplified equivalent model of universal coupling with cross shaft was established to study the relationship between angle of shafting and the vibration characteristics of shafting. Finally, the anti-load characteristics of shafting were analyzed, the bearing capacity of the unmanned ship in harsh environment was improved by controlling the parameters such as shaft angle. It was concluded that the propulsion system of unmanned ship with adjustable universal coupling is very sensitive to impact loads, by controlling the shafting speed, the shaft angle and other parameters, the load-bearing capacity of the unmanned ship can be improved.

***Keywords**: Propulsion shaft, Universal joint, Shaft vibration, Impact response.*

I. INTRODUCTION

In recent years, with the application of unmanned technology in ships, unmanned ship have gradually entered people's vision and developed rapidly. Due to the small size of unmanned ship design at present, the arrangement of propulsion shafting is difficult, and the unmanned ship may be subjected to strong impact during the voyage, which will cause violent vibration of the boat body, thus affecting the normal operation of the propulsion system. Therefore, when the propulsion shafting of unmanned ship is subjected to mechanical forces in the form of impact, sway, centrifugal acceleration, flutter and so on, its impact resistance has a very important impact on the vitality and combat effectiveness of unmanned ship. For some unique unmanned ship body structure, the boat motor can not be arranged in the underwater cylindrical submersible body, but in the water boat body structure, propeller shaft and thrust shaft are installed in the underwater submersible body, there is a large height difference between the output centerline of the motor of the boat body and the centerline of the propeller shaft, and its vertical distance is several thousand millimeters [1]. At this time, the ship shafting through a certain angle of the coupling connection, so that the two shafts continue to rotate to transfer transmission and torque.

For coupling drives with a certain dip angle, Hui Lu Technology applied finite element analysis to obtain the stress and displacement results of the elastic coupling at rated torque, the modal shapes of the first three elastic couplings and their corresponding natural frequencies [2]. C.M. Li and J.H. Li derived the rotational speed relationship between the driving shaft and the driven shaft of the universal coupling in the right-hand coordinate system according to the multi-body theory [3,4]. L.H. Xia and J.H. Huang used the structure principle of single universal joint to analyze its motion, and simulated its motion based on UG software [5,6]. Y.F. Hu established the torsional vibration calculation model of the propulsion shafting of MTU diesel engine, and analyzed the excitation characteristics and the torsional vibration characteristics of the propulsion shafting of MTU diesel engine [7]. Based on the nonlinear contact theory, Hui Wu established a contact model of a flange type hydraulic coupling to obtain the stress distribution of each component of the coupling under maximum load [8]. Zhao Guang has conducted theoretical and experimental research on the coupling components of marine power plant, providing an effective theoretical method and valuable reference for power plant design [9]. M.S. Sun used the fourth-order Runge Kutta method to simulate and numerically analyze the bending vibration and torsional vibration of shaft system [10]. L.X. Dong established a mechanical model based on the stern shaft-oil film-stern structure system, studied the variation law of the average impact force, impact amplitude, axis track and other parameters of the stern shaft under the impact load [11]. N.Q. Xiao established the equivalent model of torsional vibration by lumped parameter method, and calculated and analyzed the transient torsional vibration of a ship's propulsion shafting under ice load in time domain by Newmark-β method [12].

However, the universal joint of cross shaft type is in the process of transmitting torque, there is a certain angle between the driving shaft and the driven shaft of the coupling, even if the driving shaft speed is constant, the driven shaft will also produce speed fluctuation. There is no definite conclusion about the effect of shaft angle on shafting vibration. The requirements of anti-wave resistance and impact resistance of inclined shaft of unmanned ship are different from those of traditional technical specifications, so more attention must be paid to the reliability of the propulsion system [13,14]. Therefore, on the basis of the simplified model, the structure model of unmanned ship was established in this paper, and the influence of shaft angle on shafting vibration was analyzed. At the same time, the anti-load characteristics of the propulsion shafting were calculated, which is helpful to improve the engineering adaptability in the reliability design of unmanned ship.

II. APPLICATION OF ELECTRIC PROPULSION SYSTEM WITH VARIABLE SHAFT ANGLE

Fig 1 shows the overall structure model of the unmanned ship, and the ship is mainly composed of boat body, motor, transmission system and so on. The motor is mounted on the deck, and the propeller and thrust shaft are mounted in the submerged body. In general, electrical equipment is installed inside the boat, however, due to the small size of the ship design, the motor is moved to the deck, which can make full use of the upper space, greatly increasing the flexibility of unmanned ship design, construction and use, at the same time, it is also conducive to the maintenance and overhaul of motor equipment. Therefore, the biggest difference in structure between the electric propulsion system of this ship and the general electric propulsion system is that the shaft intersect and need to be connected through the universal joint of the cross shaft.

Forest Chemicals Review
www.forestchemicalsreview.com
ISSN: 1520-0191
September-October 2022 Page No. 1151– 1166
Article History: Received: 06 April 2022, Revised: 28 April 2022, Accepted: 04 May 2022, Publication: 31 May 2022

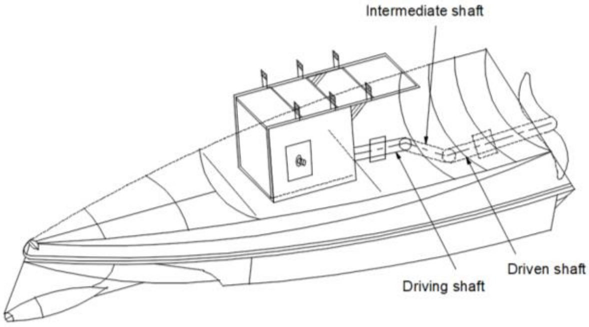

Fig 1: Structure diagram of unmanned ship

III. CONSTRUCTION OF PROPULSION SHAFTING MOTION MODEL

3.1 Establishment of Coordinate System

As shown in Fig 1, two shafts with intersecting shaft can be connected by the universal joint of cross shaft type shown in Fig 2 [15], when the driving shaft of the universal joint rotates at a constant angular speed, the motion characteristics of the driven shaft of the universal joint will be affected by the change of the shaft angle of the driven shaft of the universal joint, and in the kinematic analysis of the universal joint, the kinematic coordinate system can be established first. At present, there are two main ways to construct the kinematic coordinate system of universal joint: graphic method and coordinate transformation method, here, the kinematics coordinate system of the universal joint was established, the kinematic relation of the universal joint was deduced by the coordinate transformation method, which lays a certain foundation for the following vibration analysis.

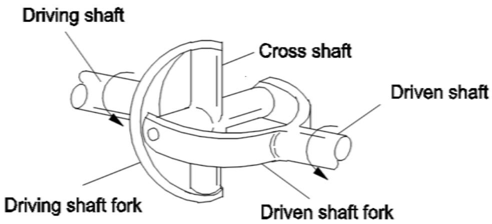

Fig 2: Structure drawing of universal joint of cross shaft type

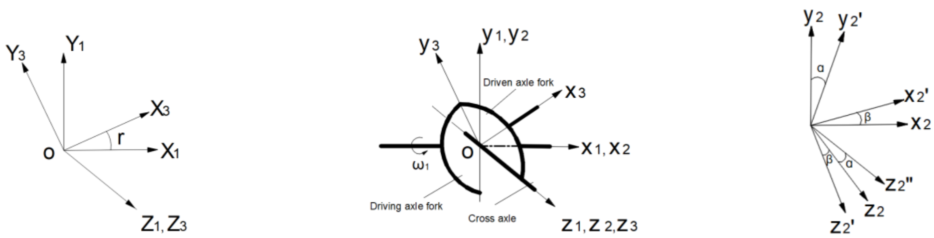

(a) (b) (c)

Fig 3: Coordinate system of universal joint of cross shaft type

Forest Chemicals Review
www.forestchemicalsreview.com
ISSN: 1520-0191
September-October 2022 Page No. 1151– 1166
Article History: Received: 06 April 2022, Revised: 28 April 2022, Accepted: 04 May 2022, Publication: 31 May 2022

Establish the kinematic coordinate system shown in Fig 3, in Fig 3(a), $oX_1Y_1Z_1$ and $oX_3Y_3Z_3$ are the fixed coordinate systems of the driving shaft and the driven shaft, respectively. In Fig 3(b), $ox_1y_1z_1$, $ox_2y_2z_2$ and $ox_3y_3z_3$ are the initial coordinate systems of the driving shaft, cross shaft and driven shaft in the universal joint structure, respectively. Fig 3(c) shows the coordinates of the cross shaft before and after the movement. The coordinate system $ox_2{'}y_2{'}z_2{'}$ can be regarded as the initial coordinate system $ox_2y_2z_2$ rotating α to $ox_2y_2{'}z_2{''}$in the direction of ox_2, and then rotating β to $ox_2{'}y_2{'}z_2{'}$ in the direction of $oy_2{'}$.

According to Fig 3(a), through Euler coordinate transformation, the relationship between fixed coordinate systems $oX_1Y_1Z_1$ and $oX_3Y_3Z_3$ can be expressed as follows

$$\begin{bmatrix} \mathrm{cosr} & -\mathrm{sinr} & 0 \\ \mathrm{sinr} & \mathrm{cosr} & 0 \\ 0 & 0 & 1 \end{bmatrix} \begin{bmatrix} X_3 \\ Y_3 \\ Z_3 \end{bmatrix} = \begin{bmatrix} X_1 \\ Y_1 \\ Z_1 \end{bmatrix} \tag{1}$$

When the driving shaft of the universal joint rotates at equal angular velocity $\dot{\theta}_1$, the dynamic coordinate system can be expressed as

$$\begin{bmatrix} 1 & 0 & 0 \\ 0 & cos\theta_1 & -sin\theta_1 \\ 0 & sin\theta_1 & cos\theta_1 \end{bmatrix} \begin{bmatrix} x_1 \\ y_1 \\ z_1 \end{bmatrix} = \begin{bmatrix} X_1 \\ Y_1 \\ Z_1 \end{bmatrix} \tag{2}$$

$$\begin{bmatrix} 1 & 0 & 0 \\ 0 & cos\theta_3 & -sin\theta_3 \\ 0 & sin\theta_3 & cos\theta_3 \end{bmatrix} \begin{bmatrix} x_3 \\ y_3 \\ z_3 \end{bmatrix} = \begin{bmatrix} X_3 \\ Y_3 \\ Z_3 \end{bmatrix} \tag{3}$$

After rotation, the dynamic coordinate system $ox_2y_2z_2$ can be expressed as the coordinate system $oX_1Y_1Z_1$

$$\begin{bmatrix} X_1 \\ Y_1 \\ Z_1 \end{bmatrix} = \begin{bmatrix} cos\beta & 0 & sin\beta \\ 0 & 1 & 0 \\ -sin\beta & 0 & cos\beta \end{bmatrix} \begin{bmatrix} 1 & 0 & 0 \\ 0 & cos\alpha & -sin\alpha \\ 0 & sin\alpha & cos\alpha \end{bmatrix} \begin{bmatrix} x_2 \\ y_2 \\ z_2 \end{bmatrix} \tag{4}$$

By introducing equation (2) into equation (1), the kinematic relationship among driving shaft, driven shaft and shaft angle can be obtained

$$\begin{bmatrix} 1 & 0 & 0 \\ 0 & cos\theta_1 & -sin\theta_1 \\ 0 & sin\theta_1 & cos\theta_1 \end{bmatrix} \begin{bmatrix} x_1 \\ y_1 \\ z_1 \end{bmatrix} = \begin{bmatrix} cosr & -sinr & 0 \\ sinr & cosr & 0 \\ 0 & 0 & 1 \end{bmatrix} \begin{bmatrix} 1 & 0 & 0 \\ 0 & cos\theta_3 & -sin\theta_3 \\ 0 & sin\theta_3 & cos\theta_3 \end{bmatrix} \begin{bmatrix} x_3 \\ y_3 \\ z_3 \end{bmatrix} \tag{5}$$

3.2 Analysis of Motion Characteristics of Shafting

When the driving shaft of the universal joint of cross shaft type rotates at equal angular velocity $\dot{\theta}_1$, how the motion characteristics of the universal joint will change with the change of the shaft angle of the cross shaft needs further analysis through formula derivation.

Forest Chemicals Review
www.forestchemicalsreview.com
ISSN: 1520-0191
September-October 2022 Page No. 1151– 1166
Article History: Received: 06 April 2022, Revised: 28 April 2022, Accepted: 04 May 2022, Publication: 31 May 2022

Considering the orthogonality of the two shafts of the cross shaft, it can be obtained $\cos(y_1, z_3) = 0$, combining formula (5) has

$$\sin\theta_1\cos\theta_3 = \cos r\cos\theta_1\sin\theta_3, \text{ namely}$$
$$\tan\theta_1 = \cos r\tan\theta_3 \tag{6}$$

When the driving shaft rotates π/2, the driven shaft also rotates π/2, which can be obtained by formula (6)

$$\tan\theta_3 = \cos r\tan\theta_1 \tag{7}$$

By differentiating the time on both sides of equation (7), equation (8) was obtained

$$\dot{\theta}_3 = \frac{\mathrm{d}\theta_3}{\mathrm{dt}} = \arctan(\cos r\tan\theta_1)' = \frac{\cos r}{1-(sinr\cdot cos\theta_1)^2}\cdot\dot{\theta}_1 \tag{8}$$

Taking the derivative of equation (8) again to obtain the expression of the driven shaft acceleration

$$\dot{\theta}_3{}' = \frac{-(sinr)^2\cdot cosr\cdot sin(2\theta_1)}{(1-(sinr\cdot cos\theta_1)^2)^2}\cdot\dot{\theta}_1{}^2 + \frac{\cos r}{1-(sinr\cdot cos\theta_1)^2}\cdot\dot{\theta}_1{}' \tag{9}$$

According to equations (8) and (9), the relationship between angular velocity and acceleration of the driving and driven shafts can be obtained by programming calculation in Matlab software, as shown in Fig. 4 (a) and (b). Set the angular velocity $\dot{\theta}_1$ of the driving shaft to 3600 rad/min, and the shaft angles of the driven shaft to r = 3°, r = 5° and r = 8°, respectively. Rotating the driving shaft for 2.5 cycles, and output the fluctuation charts of the angular velocity and acceleration of the driven shaft respectively.

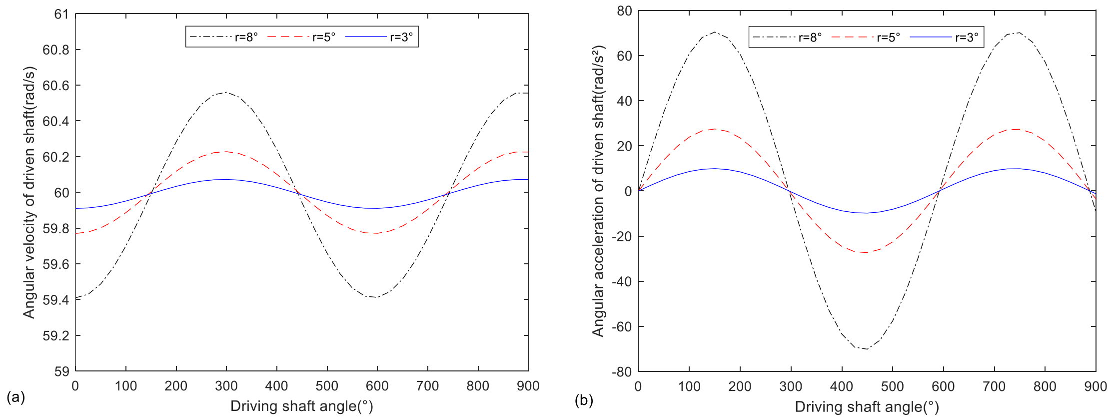

(a)Angular velocity fluctuation (b)Angular acceleration fluctuation

Fig. 4: Angular velocity and acceleration fluctuation of driven shaft under different shaft angles

Fig. 4(a) and 4(b) show that in the process of cross shaft universal joint transmission, the variation of the angular velocity and acceleration of the driven shaft at different shaft angles. Taking the driving shaft

Forest Chemicals Review
www.forestchemicalsreview.com
ISSN: 1520-0191
September-October 2022 Page No. 1151– 1166
Article History: Received: 06 April 2022, Revised: 28 April 2022, Accepted: 04 May 2022, Publication: 31 May 2022

rotating for 2.5 cycles as the observation period, the fluctuation characteristics are as follows: When the angle between the two shaft is present, the driving shaft rotates at a constant angular velocity $\dot{\theta}_1$ quarter, the angular velocity and acceleration of the driving and driven shaft are not always equal, the range of angular velocity is 60±0.6rad/s, this reflects the unequal speed motion characteristics of the universal joint of cross shaft type, it is also the cause of propulsion system vibration; And as the angle between the two shaft increases, the angular velocity and acceleration of the driven shaft fluctuate sharply, this shows that when the shaft angle is too large, the angular acceleration will be great, it will result in severe vibration of the propulsion system.

IV. ANALYSIS OF THE INFLUENCE OF SHAFT ANGLE ON SHAFTING VIBRATION

4.1 Torsional Velocity Analysis of Cross Shaft in Fixed Coordinate System

It was concluded from fig. 4 that the angular acceleration of the driven shaft of the universal joint of cross shaft type is greatly affected by the shaft angle， therefore, it can be known that the torsional angular velocity of the cross shaft in the fixed coordinate system is also affected, if the torsional angular velocity of universal joint of cross shaft type in the fixed coordinate system fluctuation sharply with the change of the shaft angle, the reliability of the propulsion system will be affected.

Will formula (3) into the formula (1), have,

$$\begin{bmatrix} \mathrm{cosr} & -\mathrm{sinr} & 0 \\ \mathrm{sinr} & \mathrm{cosr} & 0 \\ 0 & 0 & 1 \end{bmatrix} \begin{bmatrix} 1 & 0 & 0 \\ 0 & cos\theta_3 & -sin\theta_3 \\ 0 & sin\theta_3 & cos\theta_3 \end{bmatrix} \begin{bmatrix} x_3 \\ y_3 \\ z_3 \end{bmatrix} = \begin{bmatrix} \mathrm{X}_1 \\ \mathrm{Y}_1 \\ \mathrm{Z}_1 \end{bmatrix} \quad (10)$$

According to the formula (4) and formula (10), have

$$\begin{bmatrix} X_1 \\ Y_1 \\ Z_1 \end{bmatrix} = \begin{bmatrix} sinrsin\theta_3 \\ -cosrsin\theta_3 \\ cos\theta_3 \end{bmatrix} = \begin{bmatrix} sin\beta \\ -sin\alpha cos\beta \\ cos\alpha cos\beta \end{bmatrix} \quad (11)$$

By formula (6) and formula (11), there are

$$\begin{cases} \alpha = \theta_1 \\ \beta = \arctan\left(tanr \cdot sin\theta_1\right) \end{cases} \quad (12)$$

Therefore, the torsional angular velocity of the cross shaft in the fixed coordinate system can be obtained

$$\begin{cases} \dot{\theta}_{2x} = \dot{\theta}_1 \\ \dot{\theta}_{2y} = 2\dot{\beta} cos\theta_1 = \frac{sin2r \cdot (cos\theta_1)^2}{1-(sinr \cdot cos\theta_1)^2} \cdot \dot{\theta}_1 \\ \dot{\theta}_{2z} = 2\dot{\beta} sin\theta_1 = \frac{sinr \cdot cosr \cdot sin2\theta_1}{1-(sinr \cdot cos\theta_1)^2} \cdot \dot{\theta}_1 \end{cases} \quad (13)$$

Forest Chemicals Review
www.forestchemicalsreview.com
ISSN: 1520-0191
September-October 2022 Page No. 1151– 1166
Article History: Received: 06 April 2022, Revised: 28 April 2022, Accepted: 04 May 2022, Publication: 31 May 2022

When r = 3°, r = 5°, r = 8° and $\dot{\theta}_1$ =3600 rad/min,the motion curves of the cross shaft in the Y direction and Z direction of the fixed coordinate system can be obtained by formula (13), as shown in Fig 5.

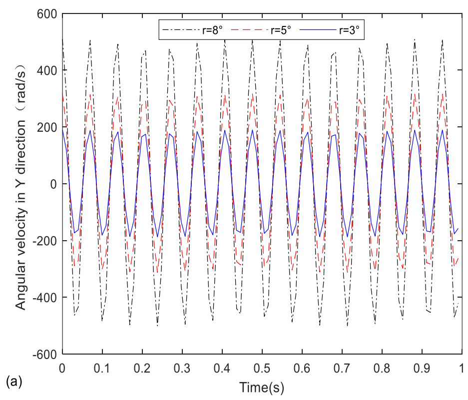

(a)Time domain diagram in Y direction

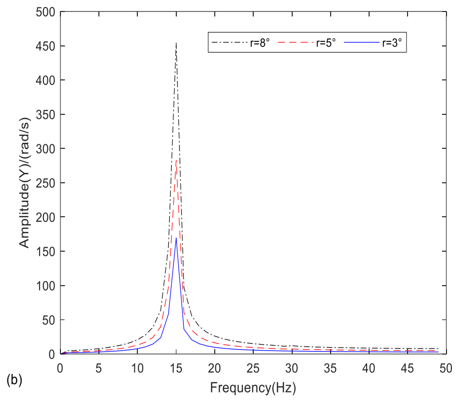

(b)Frequency domain diagram in Ydirection

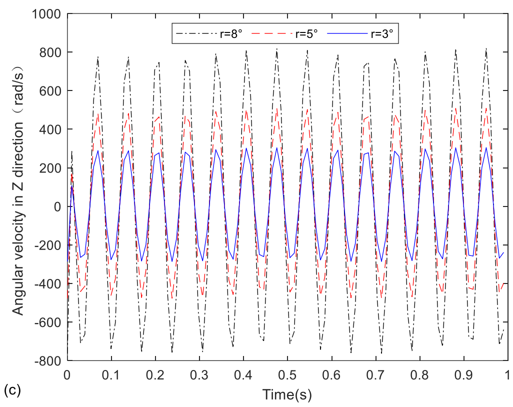

(a)Time domain diagram in Z direction

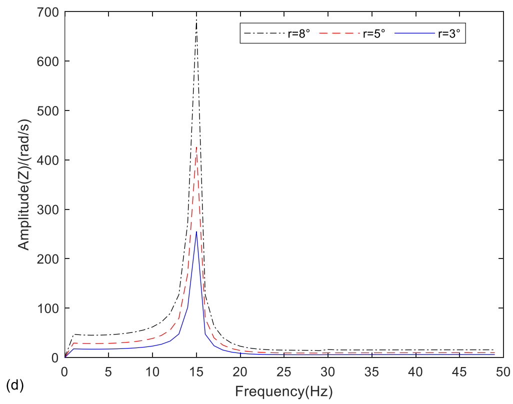

(b)Frequency domain diagram in Z direction

Fig 5: Response curves of cross shaft in Y and Z directions under different shaft angles

Fig 5(a) and 5(b) show the torsional angular velocity change of the cross shaft in the Y and Z direction during the transmission process of the cross shaft universal joint. It can be found that

(1) The torsional angular velocity diagram of the cross shaft in Y and Z direction shows a quasi-periodic change, and when the shaft angle is constant, the torsional angular velocity of the cross shaft in Z direction is higher than that in Y direction. Therefore, when using the universal joint of the cross shaft, in order to prevent the torsional angular velocity amplitude in Z direction from fluctuating excessively, the shaft angle should be controlled within an appropriate range.

(2) When the shaft angle r=3°, the torsional angular velocity of the cross shaft in Z direction is 1.5 times as much as that in Y direction, and when the shaft angle r=8°, it reaches 1.6 times, which indicates that when the shaft angle increases, the torsional angular velocity difference of the cross shaft in Y and Z direction will increase, although the velocity increase is small, it may cause vibration universal joint of the cross shaft in Y and Z direction, and then affect the stability of the system.

Forest Chemicals Review
www.forestchemicalsreview.com
ISSN: 1520-0191
September-October 2022 Page No. 1151– 1166
Article History: Received: 06 April 2022, Revised: 28 April 2022, Accepted: 04 May 2022, Publication: 31 May 2022

(3) The data in Fig 5(a) and Fig 5(c) can be transformed by FFT, and the frequency domain diagram of the torsional angular velocity of the cross shaft in Y and Z direction can be obtained. It can be seen that in the low frequency range of 0-25Hz, the amplitude corresponding to different angles decreases with the increase of frequency, and the abscissa corresponding to the main peak is concentrated at 15Hz, indicating that at this frequency, the increase of the shaft angle has the greatest influence on the movement of the cross shaft in Y and Z direction.

4.2 Torsional Vibration Analysis

In the process of torque transmission, because there is a shaft angle between the driving shaft and the driven shaft, it can be seen from the conclusion in Fig. 4 and Fig. 5 that even if the driving shaft drives at a angular velocity $\dot{\theta}_1$, when the shaft angle changes, the angular acceleration of the driven shaft will fluctuate and the stability of the propulsion system is also affected [16], and there is no clear conclusion as to how the shaft angle affects the vibration of the shaft system. The change of shaft angle may lead to the aggravation of torsional vibration of driven shaft, and then bring harm to the safe operation of the whole shaft system. Therefore, the influence of the change of shaft angle on torsional vibration of shaft system was considered here.

According to Fig 1, a simplified equivalent model of universal joint of the double cross shaft was established, as shown in Fig 6

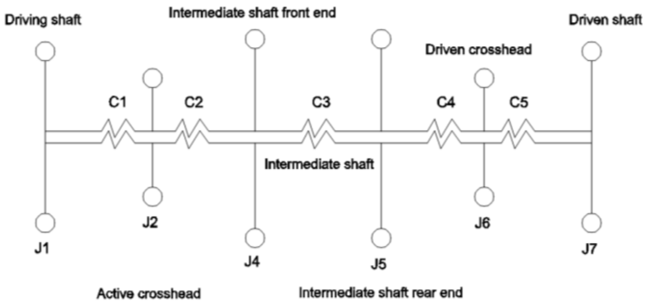

Fig 6: Equivalent model of universal joint of the double cross shaft

Kinetic energy of universal joint of the cross shaft is

$$E_p = (J_1\dot{\theta}_1{}^2 + J_2\dot{\theta}_2{}^2 + J_4\dot{\theta}_4{}^2 + J_5\dot{\theta}_5{}^2 + J_6\dot{\theta}_6{}^2 + J_7\dot{\theta}_7{}^2)/2 \tag{14}$$

Potential energy is

$$E_v = \Big[c_1(\theta_1 - \theta_{2x})^2 + c_{2x}(\theta_{2x} - \theta_4 \mathrm{cosr})^2 + c_{2y}\left(\theta_{2y} - \theta_4 \mathrm{sinr}\right)^2 + c_3(\theta_4 - \theta_5)^2 + c_{4y}(\theta_5 \mathrm{cosr} - \theta_{6x})^2 + c_{4x}\left(\theta_5 \mathrm{sinr} - \theta_{6y}\right)^2 + c_5(\theta_{6x} - \theta_7)^2\Big]/2 \tag{15}$$

In the above formula, the numbers in the lower corner mark of related symbols correspond to the

Forest Chemicals Review
www.forestchemicalsreview.com
ISSN: 1520-0191
September-October 2022 Page No. 1151– 1166
Article History: Received: 06 April 2022, Revised: 28 April 2022, Accepted: 04 May 2022, Publication: 31 May 2022

symbols in Fig. 6, and the characters in the lower corner mark correspond to the coordinate axis of the fixed coordinate system in Fig 3(a).

There are

$$J_6\dot{\theta}_6{}^2 = (J_{6x}\dot{\theta}_{6x}{}^2 + J_{6y}\dot{\theta}_{6y}{}^2 + J_{6z}\dot{\theta}_{6z}{}^2) \tag{16}$$

By formula (12), and according to the symmetrical property of the cross shaft, there are

$$J_{6y} = J_{6z} \tag{17}$$

$$\begin{cases} \dot{\theta}_{6y} = \frac{sin2r\cdot(cos\theta_{6x})^2}{1-(sinr\cdot cos\theta_{6x})^2}\cdot\dot{\theta}_{6x} \\ \dot{\theta}_{6z} = \frac{sin2r\cdot sin\theta_{6x}\cdot cos\theta_{6x}}{1-(sinr\cdot cos\theta_{6x})^2}\cdot\dot{\theta}_{6x} \end{cases} \tag{18}$$

Will type (17) and (18) into the formula (16), there are

$$J_6\dot{\theta}_6{}^2 = [J_{6x} + J_{6y}(\frac{sin2r\cdot cos\theta_{6x}}{1-(sinr\cdot cos\theta_{6x})^2})^2]\cdot\dot{\theta}_{6x}{}^2 \tag{19}$$

The equation of formula (18) can be obtained by integrating both sides at the same time

$$\begin{cases} \theta_{6y} = \frac{2}{sinr}\cdot\arctan(\frac{tan\theta_{6x}}{cosr}) - \frac{2\theta_{6x}}{tanr} \\ \theta_{6z} = -\frac{1}{tanr}\cdot\ln((sinr\cdot cos\theta_{6x})^2 - 1) \end{cases} \tag{20}$$

According to Lagrange equation of the second kind, θ_1, θ_{2x}, θ_4, θ_5, θ_{6x} and θ_7 are selected as generalized coordinates, and the following differential equations of torsional motion of double universal joint of the cross shaft can be established

$$\begin{aligned}
&J_1\ddot{\theta}_1 + C_1(\theta_1 - \theta_{2x}) = 0 \\
&\left[J_{2x} + J_{2y}(\frac{\sin2r\cos\theta_{2x}}{1-(sinr)^2*(cos\theta_{2x})^2})^2\right]\ddot{\theta}_{2x} - C_1(\theta_1 - \theta_{2x}) + C_{2x}(\theta_{2x} - \theta_4\cos r) \\
&+C_{2y}\left[\frac{2}{\sin r}\arctan\left(\frac{\tan\theta_{2x}}{\cos r}\right) - \frac{2\theta_{2x}}{\tan r} - \theta_4\sin r\right]\frac{\sin2r(cos\theta_{2x})^2}{1-(sinr)^2*(cos\theta_{2x})^2} = 0 \\
&J_3\ddot{\theta}_4{}^2 + C_3(\theta_4 - \theta_5) - C_{2x}\cos r(\theta_{2x} - \theta_4\cos r) - C_{2y}\sin r[\frac{2}{\sin r}\arctan\left(\frac{\tan\theta_{2x}}{\cos r}\right) \\
&\qquad - \frac{2\theta_{2x}}{\tan r} - \theta_4\sin r] = 0 \\
&J_4\ddot{\theta}_5{}^2 - C_3(\theta_4 - \theta_5) + C_{4y}\cos r(\theta_5\cos r - \theta_{6x}) + C_{4x}\sin r[-\frac{2}{\sin r}\arctan\left(\frac{\tan\theta_{6x}}{\cos r}\right) \\
&+\frac{2\theta_{6x}}{\tan r} + \theta_4\sin r] = 0 \\
&\left[J_{5x} + J_{5y}(\frac{\sin2r\cos\theta_{6x}}{1-(sinr)^2*(cos\theta_{6x})^2})^2\right]\ddot{\theta}_{6x} - C_{4y}(\theta_5\cos r - \theta_{6x}) + C_5(\theta_{6x} - \theta_7)
\end{aligned} \tag{21}$$

Forest Chemicals Review
www.forestchemicalsreview.com
ISSN: 1520-0191
September-October 2022 Page No. 1151– 1166
Article History: Received: 06 April 2022, Revised: 28 April 2022, Accepted: 04 May 2022, Publication: 31 May 2022

$$-C_{4x}[-\frac{2}{\mathrm{sinr}}\arctan\left(\frac{\tan\theta_{6x}}{\mathrm{cosr}}\right)+\frac{2\theta_{6x}}{\mathrm{tanr}}+\theta_5\mathrm{sinr}]\ \frac{\mathrm{sin2r}(cos\theta_{6x})^2}{1-(sinr)^2*(cos\theta_{6x})^2}=\ 0$$

$$J_6\ddot{\theta}_7+C_5(\theta_{6x}-\theta_7)=0$$

It can be seen that the equations (21) contain a large number of complex trigonometric functions, so it is difficult to obtain analytical solutions. Numerical simulation can be used to analyze the vibration characteristics of the universal joint. When the driving shaft of the universal joint drives at equal angular velocity $\dot{\theta}_1$, along with the change of the initial shaft angle r, the vibration characteristics of the driven shaft are simulated by numerical simulation, which can be taken as r = 3°, r = 5°, r = 8°, and brought into the equation, and the program was written in Matlab software, and the angular displacement response curve of the driven shaft of the universal joint with the cross shaft was obtained, as shown in Fig. 7

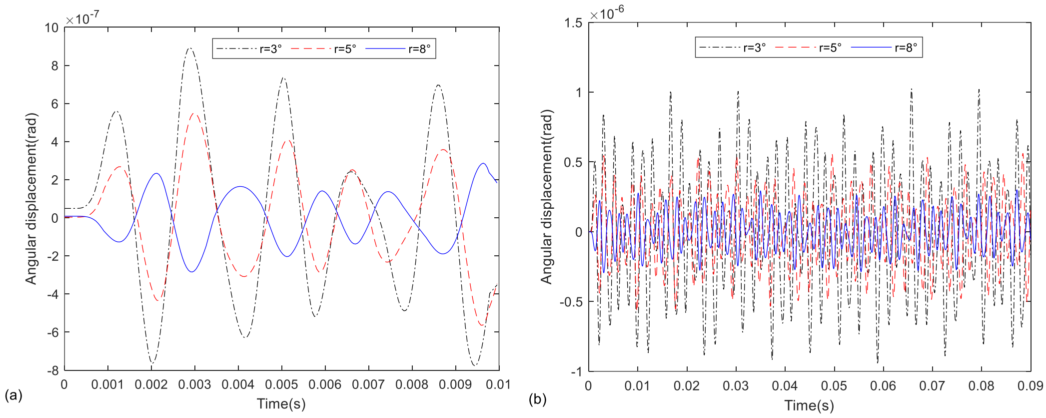

(a)(0—0.01s)　　　　　　　　(b)(0—0.09s)

Fig 7: Time domain diagram of angular displacement response of driven shaft under different shaft angles

From Fig 7, the time domain diagrams of angular displacement response of driven shaft are compared and analyzed under different shaft angles, it can be seen that when the shaft angle increases, the displacement response graph presents oscillations of different degrees .Fig 7(a) is the time domain diagram of the first 0.01s, it can be seen that when the shaft angle increases, the amplitude of the angular displacement of the driven shaft decreases, when the shaft angle increases to 8°, the displacement response graph shows a quasi-periodic change, compared with the former, the vibration amplitude is stable in the range of 0-2*10^{-7}rad, it shows that when the shaft angle increases within a certain range, the amplitude of the driven shaft changes less at the same time; In Fig 7(b), the curves start to get complicated, but the variation pattern is similar, in the case that the overall trend of the curve remains unchanged, the fluctuation of angular displacement occurs, this can be attributed to complex trigonometric functions, the amplitude of displacement response decreases with the increase of shaft angle. On the basis of Fig 7(b), the frequency domain diagram of displacement response at different angles can be obtained by fast fourier transform, as shown in Fig 8.

Forest Chemicals Review
www.forestchemicalsreview.com
ISSN: 1520-0191
September-October 2022 Page No. 1151– 1166
Article History: Received: 06 April 2022, Revised: 28 April 2022, Accepted: 04 May 2022, Publication: 31 May 2022

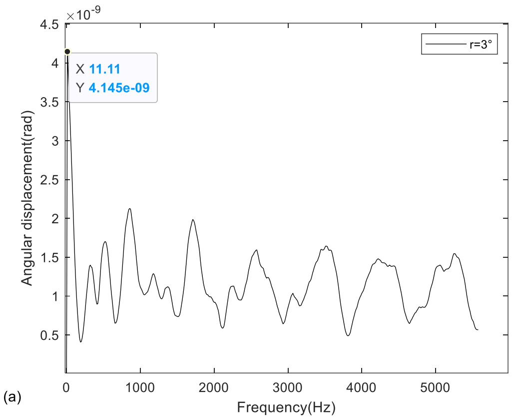

(a) r=3°

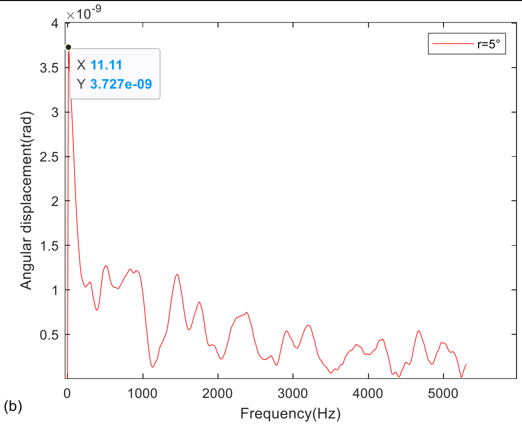

(b) r=5°

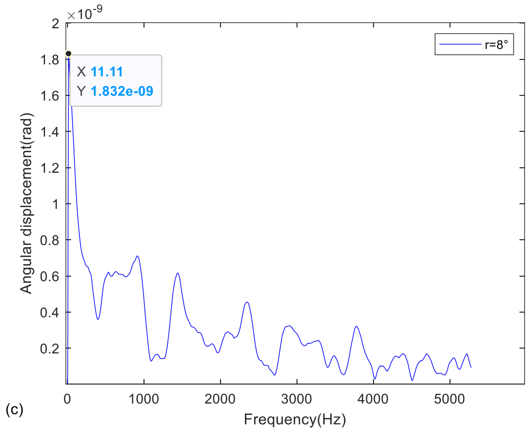

(c) r=8°

Fig. 8: Frequency domain diagram of angular displacement response of driven shaft under different shaft angles

In Fig 8, from the degree of response process, when the shaft angle increases, the amplitude of the angular displacement of the driven shaft decreases in different degrees at the same frequency, when the shaft angle increases within a certain range, the effect of angular displacement fluctuation on system stability is limited, corresponding to the conclusion in Fig. 7; In terms of the frequency of the response, in the low frequency band of 0-1000Hz, under different shaft angles, there is an obvious peak value in the initial condition, as the frequency increases, the spectrum peak falls back, it shows that angular displacement fluctuates violently in the early stage of low frequency band, and in the high frequency band above 1000Hz, as the shaft angle increases, the influence of angular displacement fluctuation decreases, spectral peak changes tend to be stable, it shows that the effect of the increase of shaft angle on angular displacement is mainly concentrated in the early stage of low frequency band, which is unfavorable to the stable operation of shafting.

V. CALCULATION OF ANTI-LOAD RESPONSE OF PROPULSION SHAFTING

The variation of the shaft angle of the universal joint of the cross shaft will affect the motion characteristics of the driven shaft. If the driven shaft is subjected to multiple external load coupling at the

Forest Chemicals Review
www.forestchemicalsreview.com
ISSN: 1520-0191
September-October 2022 Page No. 1151– 1166
Article History: Received: 06 April 2022, Revised: 28 April 2022, Accepted: 04 May 2022, Publication: 31 May 2022

same time, whether it will affect the shaft angle of the universal joint, it is also related to the stable operation of shafting [17,18]. In the current study, the analysis of vibration coupling caused by the change of shaft angle caused by axial force and flexural torque is less, therefore, the influence of axial force and flexural torque coupling on the shaft angle of the universal joint was considered here.

According to Fig 2(a), the mechanical model of universal joint of double cross shaft was established, as shown in Fig 9, the solid line represents the initial position of the intermediate shaft of the universal joint, and the dotted line represents the position of the intermediate shaft of the universal joint subjected to changes of axial force and flexural torque,the shaft angle r changes to r' and r'' respectively.

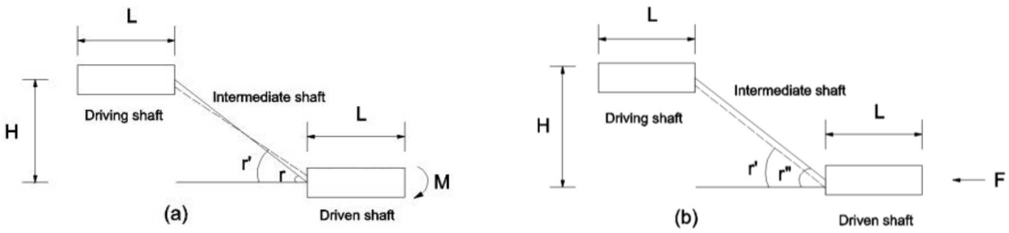

(a) Flexural torque (b) Axial vibration

Fig. 9: Mechanical model of universal joint of double cross shaft

According to the mechanical model principle, the following coupling equations can be listed

$$\begin{cases} \dfrac{H-\frac{Msin(\dot{\theta}_1 tL)}{EI}}{H} = \dfrac{sinr'}{sinr} \\ \dfrac{H}{sinr} - \dfrac{Fsin(\dot{\theta}_1 t)cosr''}{EA} = \dfrac{H}{sinr''} \end{cases} \tag{22}$$

It can be obtained from formula (13)

$$\begin{cases} \dot{\theta}_{2x} = \dot{\theta}_1 \\ \dot{\theta}_{2y} = 2\dot{\beta}cos\theta_1 = \dfrac{sin2r\cdot(cos\theta_1)^2}{1-(sinr\cdot cos\theta_1)^2}\cdot\dot{\theta}_1 \\ \dot{\theta}_{2z} = 2\dot{\beta}sin\theta_1 = \dfrac{sinr\cdot cosr\cdot sin2\theta_1}{1-(sinr\cdot cos\theta_1)^2}\cdot\dot{\theta}_1 \end{cases} \tag{23}$$

Will type (23) into the type (22), there are

$$\begin{cases} \dfrac{H-\frac{Msin\left(\dot{\theta}_{2y}\cdot\frac{1-(sinr\cdot cos\theta_1)^2}{sin2r\cdot(cos\theta_1)^2}\cdot t\cdot L\right)}{EI}}{H} = \dfrac{sinr'}{sinr} \\ \dfrac{H}{sinr} - \dfrac{Fsin(\dot{\theta}_{2z}\cdot\frac{1-(sinr\cdot cos\theta_1)^2}{sinr\cdot cosr\cdot sin2\theta_1}\cdot t)cosr''}{EA} = \dfrac{H}{sinr''} \end{cases} \tag{24}$$

To analyze the influence of coupling vibration between axial force and flexural torque on the shaft

Forest Chemicals Review
www.forestchemicalsreview.com
ISSN: 1520-0191
September-October 2022 Page No. 1151– 1166
Article History: Received: 06 April 2022, Revised: 28 April 2022, Accepted: 04 May 2022, Publication: 31 May 2022

angle of the intermediate shaft of the universal joint, taking the shaft angles of the universal joint r = 1°, r = 8° and $\dot{\theta}_1 = 3600\mathrm{rad/min}$, and using the formula (24) to write a program for calculation, it can be obtained that curves of the shaft angles r' and r "changing with time, as shown in Fig. 10 (a) and (b) respectively.

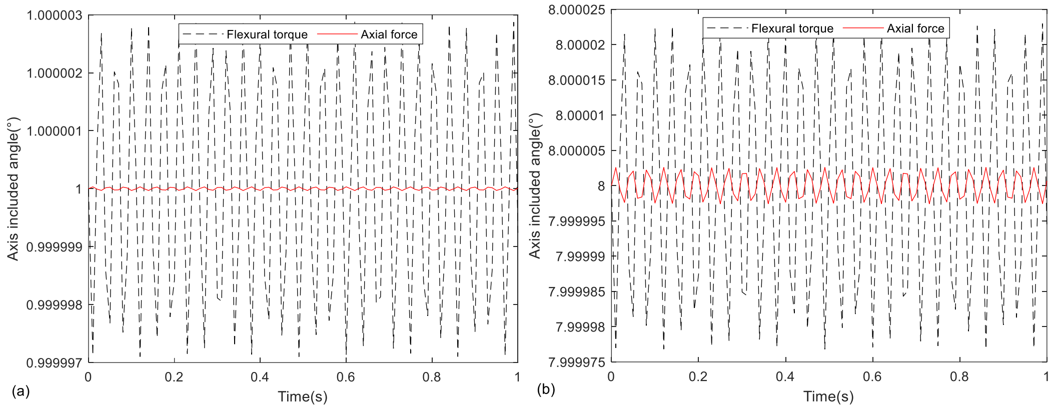

(a) r=1° (b) r=8°

Fig.10: Influence of axial force and flexural torque on shaft angle

When the driving shaft of the universal joint of the cross shaft continuously rotates at a angular velocity $\dot{\theta}_1$, it can be found from Fig. 10 that with the change of the shaft angle of the universal joint, from 0s to 1s, the influence degree of flexural torque and axial force on the shaft angle of the universal joint is different, and its characteristics are as follows

(1) when the shaft angle of the universal joint is r = 1°, the maximum influence of flexural torque on the shaft angle of the universal joint is $3*10^{-6}$ degree, while the maximum influence of axial force on the shaft angle of the universal joint is 1/30 of flexural torque, which shows that the influence of axial force on the shaft angle of the universal joint is far less than that of flexural torque.

(2) When the shaft angle of the universal joint is r = 8°, the influence of flexural torque on the shaft angle of the universal joint is still the main one, but the influence of axial force on the shaft angle of the universal joint will increase with the increase of shaft angle.

The above results show that when the driving shaft of the universal joint rotates continuously at a angular velocity $\dot{\theta}_1$, if the driven shaft is subjected to the universal joint action of axial force and flexural torque, the shaft angle of the universal joint will fluctuate. Moreover, the flexural torque has a greater influence on the shaft angle than the axial force, so the flexural torque performance of the propulsion shafting during sailing needs to be paid enough attention to.

VI. CONCLUSION

In this paper, a variable shaft angle propulsion system based on universal joint was introduced, and the influence of the change of shaft angle on the vibration characteristics of propulsion shafting was studied. Furthermore, the anti-load characteristics of propulsion shafting were analyzed as follows:

(1) In the process of torsional vibration of universal joint, when the shaft angle increases in a limited range, the amplitude of the driven shaft changes little with time, and the amplitude curve shows a

Forest Chemicals Review
www.forestchemicalsreview.com
ISSN: 1520-0191
September-October 2022 Page No. 1151– 1166
Article History: Received: 06 April 2022, Revised: 28 April 2022, Accepted: 04 May 2022, Publication: 31 May 2022

quasi-periodic variation rule; According to the frequency domain diagram of the response process, the peak frequency decreases with the increase of frequency, and the effect of increasing shaft angle on torsional vibration of the universal coupling of cross shaft is mainly concentrated in the low frequency region.

(2) The torsional velocity of the cross shaft in Y and Z direction is greatly affected by the shaft angle, according to the time domain diagram of the response process, when the shaft angle remain unchanged, the torsional velocity of the cross shaft in the Z direction is higher than that in the Y direction, in addition, when the angle increases, the difference of torsional velocity of the cross shaft in the Y and Z direction will increase; The influence of the increase of the angle on the torsional velocity of the cross shaft in the Y and Z direction is mainly concentrated in the low-frequency region, and that must be taken into account in the initial stage of ship shafting design.

(3) When the driven shaft of the universal joint of cross shaft is subjected to the coupling of axial force and flexural torque, the shaft angle will be affected, the influence of axial force on shaft angle is less than that of flexural torque. Accordingly, the influence of flexural torque on shaft angle of the universal joint will increase with the increase of the angle, and more research is needed to reveal their rule.

Appendix A:The meaning of the symbols used in this paper

Notation	
r	initial angle of intermediate shaft of coupling
θ_1	torsion angle of driving shaft
θ_3	torsion angle of driven axle fork
α and β	rotation angle of coordinate system
θ_{2x} and θ_{2y}	torsion angle of driving crosshead in x and y directions
θ_{2z}	torsion angle of driving crosshead in z direction
θ_4 and θ_5	torsion angle of front and rear ends of intermediate shaft
θ_6	torsion angle of driven crosshead
θ_7	torsion angle of driven shaft
J_1	rotational inertia of driving shaft
J_2	rotational inertia of driving crosshead
J_{2x} and J_{2y}	rotational inertia of driving crosshead in horizontal and vertical directions
J_4	moment of inertia at the front end of intermediate shaft
J_5	moment of inertia at the rear end of intermediate shaft
J_6	rotational inertia of driven crosshead
J_7	rotational inertia of driven shaft
E_P and E_v	kinetic energy and potential energy of coupling
C_1	direct contact stiffness of driving axle fork and cross axle

C_{2x}	horizontal contact stiffness of driving axle fork and cross shaft
C_{2y}	contact stiffness of driving axle fork and cross axle in vertical direction
C_3	torsional stiffness of intermediate shaft
C_{4x}	contact stiffness of driven axle fork and cross axle in horizontal direction
C_{4y}	contact stiffness of driven axle fork and cross axle in vertical direction
C_5	direct contact stiffness between driven axle fork and cross axle
r' and r"	angle change of intermediate shaft of coupling
L	length of driving shaft and driven shaft of coupling
H	vertical distance between driving and driven shafts
M	bending moment of driven shaft of coupling
F	axial force on driven shaft of coupling
A	cross-sectional area of coupling intermediate shaft

ACKNOWLEDGEMENTS

This research was supported by Zhejiang Provincial Natural Science Foundation of China under Grant No. LY20E090002.

REFERENCES

[1] G.Y. Cai, Transmission characteristics of power plant of catamaran in small waterplane. Guangdong shipbuilding, 2002(01):16-20

[2] H. Lu, C.H. Ding, Z.B. Huo, G.H. Zhang, Static characteristic analysis of large torque elastic coupling. Mechanical Transmission, 2011,35(10):16-20

[3] C.M. Li, Modification of the speed ratio formula of universal coupling and the calculation formula of belt drive pressure. World Science and Technology Research and Development, 2008(01):38-41

[4] J.H. Li, W.B. Wang, L.F. Lou, Y.P. Wang, Study on rigid-flexible coupling dynamics of double cross joint. Mechanical transmission, 2016, 40 (10): 33-37

[5] L.H. Xia, Motion analysis and simulation of universal coupling based on UG software. equipment manufacturing technology, 2013(04):45-46

[6] J.H. Huang, Motion Simulation of Double Universal Coupling. Journal of Donghua University (Natural Science Edition), 2011, 37(04):506-508

[7] Y.F. Hu, R.P. Zhou, Yong Xu, Z.Q. Zhu, Coupling matching research and torsional vibration characteristics prediction of MTU diesel engine propulsion shafting. China Ship Research, 2019, 14(04):120-127

[8] H. Wu, S.W. Zhou, Impact resistance analysis of flanged hydraulic couplings. Ship Science and Technology, 2015, 37(07):38-42

[9] G. Zhao, Z.S. Liu, Feng Chen, Y.L. Wang , Experimental study on misalignment and frequency locking fault of rotor-coupling-bearing-isolator system. Journal of Dynamics and Control, 2009, 7(02):171-176

[10] M.S. Sun, Study on bending-torsion coupling vibration of main shaft system of hydropower unit caused by hydraulic factors. North China University of Science and Technology, 2017

[11] L.X. Dong,Yi Yang, J.K. Gao, Y.P. Gong, Research on collision load response based on ship stern shaft-oil film-stern structure system. China Ship Research, 2017, 12(01):122-127
[12] N.Q. Xiao, Xiang Xu, R.P. Zhou, Calculation of transient torsional vibration of ship shafting in ice area and software development. China Shipbuilding, 2019, 60(02):138-149
[13] L.X. Dong, Y.S. Niu, Qiang Yuan, M.Y. Yang, Calculation of shock response of electric propulsion unmanned ship shafting. Ship Science and Technology, 2021, 43(17):108-111
[14] Y. Wang, G.X. Wang, Dynamic Simulation of Impact Resistance of Ship Systems and Equipment. Computer Simulation, 1999(01):29-31
[15] K. Vijayan, C.R Barik, O.P. Sha, Shock transmission through universal joint of cutter suction dredger. Ocean Engineering, 2021, 233
[16] D.F. Zhang, Research and optimization of dynamic characteristics of a certain type of passenger car transmission shaft assembly. Zhengzhou University, 2020
[17] Y.S. Pan, Han Li, Force analysis of double-cross universal joint intermediate shaft of automobile steering system. Transmission technology, 2020,34(01):37-43
[18] X.F. Wen, B.G. Cai, X.D. Wang, Numerical simulation of ship propulsion shafting under cyclic load. China Navigation, 2021,44(03):13-19